Successive-Interference-Cancellation-Free NOMA for Indoor VLC: A Generalized Spatial Modulation Based Approach

Tengjiao Wang[1], Fang Yang[1,2], Changyong Pan[1,2], Jian Song[1,2], and Zhu Han[3,4]
[1]Department of Electronic Engineering, Tsinghua University,
Beijing National Research Center for Information Science and Technology (BNRist), Beijing 100084, P. R. China
[2]Key Laboratory of Digital TV System of Guangdong Province and Shenzhen City,
Research Institute of Tsinghua University in Shenzhen, Shenzhen 518057, P. R. China
[3]University of Houston, Houston, TX 77004, USA
[4]Department of Computer Science and Engineering, Kyung Hee University, Seoul, South Korea

***Abstract*—Recently, visible light communication (VLC) has been regarded as one promising candidate to complement the conventional radio frequency communication in the future communication systems. In this paper, a novel successive-interference-cancellation-free non-orthogonal multiple access (NOMA) scheme is proposed for indoor VLC systems, based on the generalized spatial modulation technique. Different from the conventional NOMA schemes, information bits for users with diverse quality of service requirements are conveyed through different domains of the transmitted signals. Therefore, the intra-group interference among users is canceled and the successive interference cancellation is avoided to reduce the computational complexity at the receiver side. Theoretical analysis and simulation results are further provided to validate the superior performance of the proposed scheme over conventional orthogonal and non-orthogonal multiple access schemes.**

***Index Terms*—Visible light communication, successive interference cancellation, quality of service, generalized spatial modulation, non-orthogonal multiple access.**

I. Introduction

Visible light communication (VLC) has been emerging as a compelling technology to supplement the traditional radio frequency communication [1]. With the rapid growth of electronic devices worldwide, the future wireless communication systems are required to accommodate users with diverse quality of service (QoS) requirements [2]. In the future VLC systems, the smart electronic devices with high data rate requirements and sufficient computing resources, and the massive Internet of Things (IoT) [3] devices with low data rate requirements and limited computing capabilities are two kinds of the widely considered user devices [4]. They are also typical users for the enhanced mobile broadband (eMBB) and massive machine type communication (mMTC) scenarios in the 5G communication systems [5].

In the literature, non-orthogonal multiple access (NOMA) has been proposed to improve system capacity and guarantee massive connection [6], which also shows potentials for accommodating users with diverse QoS requirements [2]. Different from the conventional orthogonal multiple access (OMA) techniques, NOMA allocates non-orthogonal resources to user devices to improve overall channel capacity. In NOMA, successive interference cancellation (SIC) is widely used at the receiver side to enable robust signal detection [7]. However, the utilization of SIC involves high computing complexity, which is not friendly to the IoT users with limited computing capacities and power [8].

Recently, the multiple-input multiple-output (MIMO) technique has been introduced to VLC, which makes use of multiple light emitting diodes (LEDs) to improve spectral efficiencies. As an extension of the MIMO technique, the generalized spatial modulation (GenSM) technique, which maps the data information on both the spatial-domain symbols and the constellation-domain symbols, has proven to be more robust to the channel correlation in indoor VLC systems compared to conventional spatial multiplexing MIMO technology [9]. As a result, GenSM has attracted numerous research efforts in VLC, including constellation arrangement [10], dimming control [11], and precoding design [12].

In our previous work [13], [14], we have proposed several schemes for indoor VLC systems, where only one LED is considered. In this paper, we focus on the multiple access problem of the indoor multi-LED multi-user VLC systems. The contributions of this paper are multifold. 1) A novel SIC-free NOMA scheme is proposed for the indoor multi-LED multi-user VLC systems to accommodate diverse QoS requirements of the user devices, especially the smart electronic devices with high data rate demands and sufficient computing resources, and the IoT devices with low data rate requirements and limited computing capabilities. The user devices are divided into groups according to their QoS requirements. 2) With GenSM, the data information for the users with different data rate requirements can be transmitted through the spatial-domain symbols and the constellation-domain symbols, respectively. Therefore, the intra-group interference is canceled and the complicated SIC detector is avoided at the receiver. 3) A closed form approximation of the achievable rate is derived to provide efficient estimation of the achievable rate of the proposed scheme. 4) Simulation

978-1-7281-7440-2/20/$31.00 ©2020 IEEE
Authorized licensed use limited to: Tsinghua University. Downloaded on August 27,2020 at 08:36:10 UTC from IEEE Xplore. Restrictions apply.

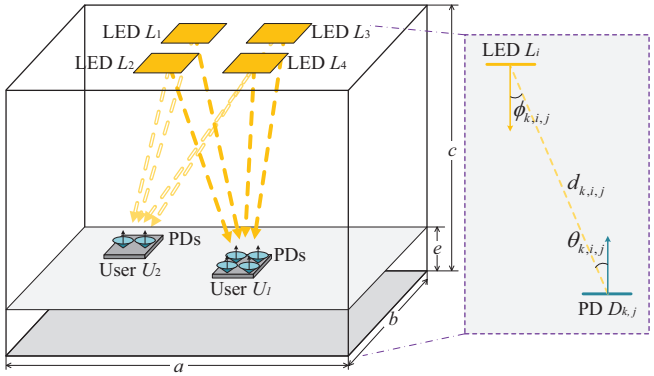


Fig. 1. The geometry setup of the indoor multiuser VLC system with multiple LEDs and multiple PDs.

results validate the superior achievable sum rate of the proposed NOMA scheme over conventional multiple access schemes.

The remainder of the paper is organized as follows. In Section II, the system model of the indoor multiuser VLC system with multiple LEDs and multiple photo-detectors (PDs) is provided. Section III and Section IV focus on the principle and the achievable rate analysis of the proposed scheme, respectively. Numerical simulation results are provided in Section V to show the performance of the proposed scheme. Finally, the paper is concluded in Section VI.

II. System Model

We consider an indoor multiuser VLC system with multiple LEDs and multiple PDs. There are N_t LEDs placed on the ceiling pointing straight down, which are denoted as L_j $(j = 1, 2, \cdots, N_t)$. K users U_k $(k = 1, 2, \cdots, K)$ are supported in the system and each user is equipped with $N_{k,r}$ PDs pointing straight up. The i-th PD equipped on the k-th user is denoted as $D_{k,i}$ $(i = 1, 2, \cdots, N_{k,r})$. The distance between the j-th LED L_j and the i-th PD on the k-th user $D_{k,i}$ is denoted as $d_{k,i,j}$, and the corresponding angle of irradiance and the angle of incidence are denoted as $\phi_{k,i,j}$ and $\theta_{k,i,j}$, respectively.

An illustration of the geometry setup with $N_t = 4$ LEDs and $K = 2$ users is shown in Fig. 1. In the indoor VLC system, the length, width, and height of the cubic room are denoted as a, b, and c, respectively. Two user terminals, U_1 and U_2 are placed on the tables with height e above the ground. U_1 and U_2 are equipped with $N_{1,r} = 4$ PDs and $N_{2,r} = 2$ PDs pointing straight up to receive the optical signals, respectively.

Mathematically, the received signals at the PDs of user U_k can be modeled as

$$\mathbf{y}_k = \gamma_k \mathbf{H}_k \mathbf{x} + \mathbf{w}_k, \tag{1}$$

where $\mathbf{x} = [x_1, x_2, \cdots, x_{N_t}]^{\mathrm{T}}$ represents the transmitted signals from the LEDs, $\mathbf{y}_k = [y_1, y_2, \cdots, y_{N_{k,r}}]^{\mathrm{T}}$ represents the received signals at user U_k, and γ_k represents the responsivity of the PDs at user U_k. $\mathbf{w}_k = [w_1, w_2, \cdots, w_{N_{k,r}}]^{\mathrm{T}}$ denotes the noise at user U_k, which is the sum of the ambient light shot noise and the thermal noise. It can be modeled as real additive white Gaussian noise (AWGN) $\mathcal{N}(\mathbf{0}, \sigma^2_{\mathrm{AWGN}}\mathbf{I}_{N_{k,r}})$ according to the central limit theorem [10], [15]. $\mathbf{H}_k$ denotes the optical channel matrix at U_k, which can be further given as

$$\mathbf{H}_k = \begin{bmatrix} h_{k,1,1} & h_{k,1,2} & \cdots & h_{k,1,N_t} \\ h_{k,2,1} & h_{k,2,2} & \cdots & h_{k,2,N_t} \\ \vdots & \vdots & h_{k,i,j} & \vdots \\ h_{k,N_{k,r},1} & h_{k,N_{k,r},2} & \cdots & h_{k,N_{k,r},N_t} \end{bmatrix}, \tag{2}$$

where $h_{k,i,j}$ denotes the optical channel gain from LED L_j to PD $D_{k,i}$. We assume the reflections from the walls, ceiling, and floors are not significant and only consider the line-of-sight (LOS) channel in this paper [16], [17]. According to [16], the optical channel gain is given as below

$$h_{k,i,j} = \begin{cases} \frac{(l+1)A}{2\pi d^2_{k,i,j}} \cos^l(\phi_{k,i,j}) \cos(\theta_{k,i,j}), 0 \le \theta_{k,i,j} \le \Theta_{1/2} \\ 0, \qquad\qquad\qquad\qquad \theta_{k,i,j} > \Theta_{1/2} \end{cases}, \tag{3}$$

where A and $\Theta_{1/2}$ represent the area and the half-power field-of-view (FOV) angle of the PDs, respectively. l represents the Lambert's mode number $l = -\ln 2 / \ln(\cos \Phi_{1/2})$, where $\Phi_{1/2}$ is the half-power angle of the LEDs.

III. Proposed SIC-Free NOMA Scheme

In this section, the novel SIC-free NOMA scheme for indoor VLC is proposed. The block diagram of the proposed scheme is illustrated in Fig. 2.

At the transmitter, we divide the supported users into groups of two users based on their QoS requirements. In each group, one user is a smart electronic device with high data rate demands, which is denoted as U_1; and the other is an IoT device with low QoS requirements, which is denoted as U_2. We can implement the user grouping through many state-of-the-art user grouping methods [18], [19]. Customized and efficient user grouping needs future research efforts.

Non-orthogonal resource allocations are adopted within each user group. Different from the conventional NOMA schemes which utilize power-domain diversities to implement multiple access, we propose a novel GenSM-based methods to cancel the intra-group interference and avoid the use of SIC. We adopt orthogonal multiple access strategies among user groups. For example, we can assign different frequency ranges to different user groups. We can also implement the orthogonal multiple access through careful design of the FOVs of PDs and the half-power angle of LEDs, so that each user group can be served by certain LEDs.

At the transmitter side, based on the principle of GenSM, only N_a LEDs are activated at the same time to transmit optical signals. Thus, $N_c = \binom{N_t}{N_a}$ spatial-domain symbols Ψ_m $(m = 1, 2, \cdots, N_c)$ can be chosen to carry information. We modulate the information bits intended for U_2 on the spatial-domain symbols. Therefore, $B_2 = \lfloor \log_2 \binom{N_t}{N_a} \rfloor$ bits

Authorized licensed use limited to: Tsinghua University. Downloaded on August 27,2020 at 08:36:10 UTC from IEEE Xplore. Restrictions apply.

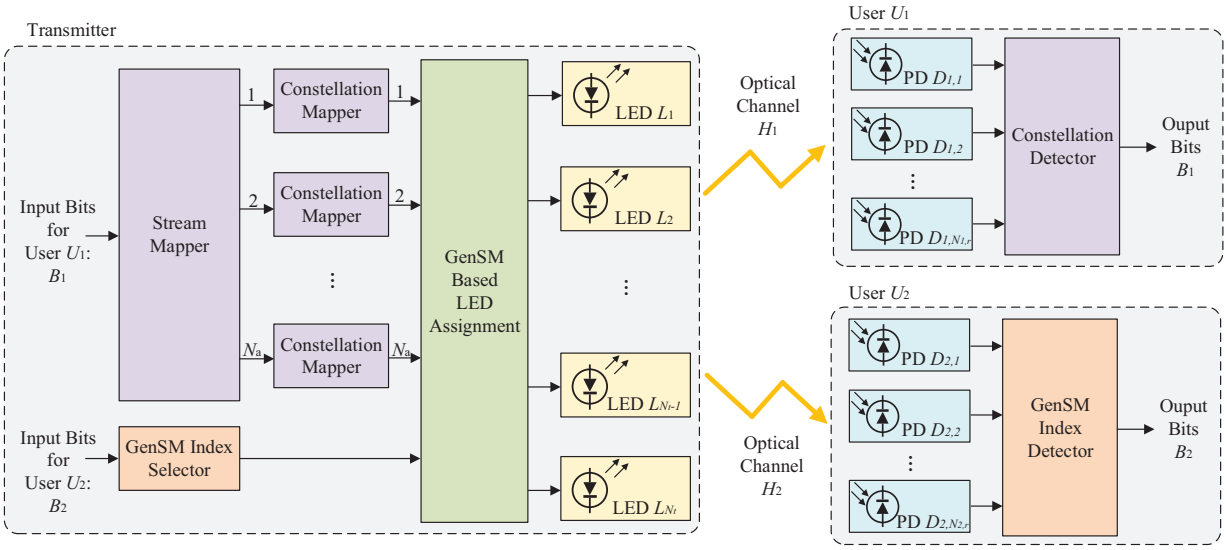


Fig. 2. The block diagram of the proposed SIC-free NOMA scheme for VLC.

can be transmitted through each spatial-domain symbol. On the other hand, we modulate the information bits intended for U_1 on the constellation-domain symbols. The information bits are split into N_a data streams and each stream is modulated according to an M-order modulation constellation. Thus, $B_1 = N_a \log_2(M)$ bits can be transmitted through each constellation-domain symbol. Therefore, the transmitted signal vectors with N_a non-zero elements can be expressed as

$$\mathbf{x} = [0, \cdots, 0, x_{\psi_1}, 0, \cdots, 0, x_{\psi_2}, \cdots, x_{\psi_{N_a}}, 0, \cdots, 0], \quad (4)$$

where $\psi_q \in [1, N_t]$ $(q = 1, 2, \cdots, N_a)$ denotes the position of the activated LEDs.

At the receiver side, the users with different QoS requirements and computing capacities can utilize different kinds of detectors. For the IoT device U_2 with limited computing capacities, simple index detectors, such as maximum ratio combining (MRC) can be adopted to estimate the required spatial-domain information. For the smart electronic device U_1 with sufficient computing capacities, it is supposed to apply a more complicated constellation detector to demodulate the constellation-domain symbols. Different from the conventional NOMA schemes, in the proposed SIC-free NOMA scheme, the intra-group interference between the users are canceled completely. Thus, there is no need to apply SIC in the proposed scheme. In conventional NOMA schemes, SIC requires the user with better channel conditions to decode the information intended for the user with poorer channel conditions first and subtract it from the received signals, which involves a lot of computations and causes error propagation. Therefore, the proposed scheme can simplify the detectors and reduce the computational complexity, which is more acceptable to the IoT devices with limited computing capacities.

IV. Achievable Rate Analysis

In this section, we analyze the achievable rate of the proposed SIC-free NOMA scheme in each user group. Firstly, we analyze the mutual information of the proposed scheme. Then, a closed form expression of the lower bound of the achievable rate is derived based on the mutual information analysis. At last, a closed form approximation of the achievable rate is further derived to obtain a better description of the achievable rate.

A. Mutual Information Analysis

Because of the chain rule of the mutual information [20], the mutual information for the two users between the transmitted signals and the received signals can be expressed as

$$\mathcal{I}(\mathbf{x}; \mathbf{y}_1) = \mathcal{I}(\mathbf{x}^{\mathrm{c}}; \mathbf{y}_1 | \mathbf{x}^{\mathrm{i}}) + \mathcal{I}(\mathbf{x}^{\mathrm{i}}; \mathbf{y}_1), \quad (5)$$

and

$$\mathcal{I}(\mathbf{x}; \mathbf{y}_2) = \mathcal{I}(\mathbf{x}^{\mathrm{c}}; \mathbf{y}_2 | \mathbf{x}^{\mathrm{i}}) + \mathcal{I}(\mathbf{x}^{\mathrm{i}}; \mathbf{y}_2), \quad (6)$$

where $\mathbf{x}^{\mathrm{c}}$ and $\mathbf{x}^{\mathrm{i}}$ denote the constellation-domain signals and the spatial-domain signals, respectively. Thus, the mutual information for the users can be divided into two parts, the spatial-domain mutual information $\mathcal{I}(\mathbf{x}^{\mathrm{i}}; \mathbf{y}_k)$ and the constellation-domain mutual information $\mathcal{I}(\mathbf{x}^{\mathrm{c}}; \mathbf{y}_k | \mathbf{x}^{\mathrm{i}})$.

In the proposed scheme, only the constellation-domain information is intended for the first user U_1. According to [21], on condition that the spatial-domain symbol is chosen, the constellation-domain mutual information can be given as

$$\mathcal{I}(\mathbf{x}^{\mathrm{c}}; \mathbf{y}_1 | \mathbf{x}^{\mathrm{i}} = \Psi_m) = \sum_{n \in \Psi_m} \log_2 \left(1 + \frac{\gamma^2 \sigma_{m,n}^2 P_{m,n}}{N_0 W} \right), \quad (7)$$

Authorized licensed use limited to: Tsinghua University. Downloaded on August 27,2020 at 08:36:10 UTC from IEEE Xplore. Restrictions apply.

$$
\begin{aligned}
\mathcal{I}(\mathbf{x}^{\mathrm{i}};\mathbf{y}_2) &= \frac{1}{N_c}\sum_{m=1}^{N_c}\int_{\mathbf{y}_2} f(\mathbf{y}_2|\mathbf{x}^{\mathrm{i}}=\Psi_m)\times\log_2\left(\frac{f(\mathbf{y}_2|\mathbf{x}^{\mathrm{i}}=\Psi_m)}{f(\mathbf{y}_2)}\right)\mathrm{d}\mathbf{y}_2\\
&= \frac{1}{N_c}\sum_{m=1}^{N_c}\left(\int_{\mathbf{y}_2} f(\mathbf{y}_2|\mathbf{x}^{\mathrm{i}}=\Psi_m)\times\log_2 f(\mathbf{y}_2|\mathbf{x}^{\mathrm{i}}=\Psi_m)\mathrm{d}\mathbf{y}_2-\int_{\mathbf{y}_2} f(\mathbf{y}_2|\mathbf{x}^{\mathrm{i}}=\Psi_m)\times\log_2 f(\mathbf{y}_2)\mathrm{d}\mathbf{y}_2\right)\\
&= \frac{1}{N_c}\sum_{m=1}^{N_c}\left(-N_{2,r}\log_2(\pi e)-\log_2(|\Sigma_m|)-\int_{\mathbf{y}_2} f(\mathbf{y}_2|\mathbf{x}^{\mathrm{i}}=\Psi_m)\times\log_2\left(\frac{1}{N_c}\sum_{t=1}^{N_c} f(\mathbf{y}_2|\mathbf{x}^{\mathrm{i}}=\Psi_t)\right)\mathrm{d}\mathbf{y}_2\right)\\
&\geq \frac{1}{N_c}\sum_{m=1}^{N_c}\left(-N_{2,r}\log_2(\pi e)-\log_2(|\Sigma_m|)-\log_2\left(\frac{1}{N_c}\sum_{t=1}^{N_c}\int_{\mathbf{y}_2} f(\mathbf{y}_2|\mathbf{x}^{\mathrm{i}}=\Psi_m)\times f(\mathbf{y}_2|\mathbf{x}^{\mathrm{i}}=\Psi_t)\right)\mathrm{d}\mathbf{y}_2\right)\\
&= \frac{1}{N_c}\sum_{m=1}^{N_c}\left(-N_{2,r}\log_2(\pi e)-\log_2(|\Sigma_m|)+N_{2,r}\log_2(\pi)-\log_2\left(\frac{1}{N_c}\sum_{t=1}^{N_c}\frac{1}{|\Sigma_m+\Sigma_t|}\right)\right)\\
&= \log_2\left(\frac{N_c}{e^{N_{2,r}}}\right)-\frac{1}{N_c}\sum_{m=1}^{N_c}\log_2\left(\sum_{t=1}^{N_c}\frac{|\Sigma_m|}{|\Sigma_m+\Sigma_t|}\right)
\end{aligned}
\tag{13}
$$

where $\sigma_{m,n}$ represents the n-th singular value of the activated sub-channel matrix with the spatial-domain symbol Ψ_m. $P_{m,n}$ represents the electrical power allocated to the n-th sub-channel in Ψ_m. N_0 and W denote the power density and bandwidth of the AWGN, respectively. Supposing the input bits are selected arbitrarily, the spatial-domain symbols are selected with equal probability. Therefore, the mutual information for U_1 can be expressed as

$$
\begin{aligned}
\mathcal{I}(\mathbf{x}^{\mathrm{c}};\mathbf{y}_1|\mathbf{x}^{\mathrm{i}}) &= \sum_{m=1}^{N_c}\Pr(\mathbf{x}^{\mathrm{i}}=\Psi_m)\times\mathcal{I}(\mathbf{x}^{\mathrm{c}};\mathbf{y}_1|\mathbf{x}^{\mathrm{i}}=\Psi_m)\\
&= \frac{1}{N_c}\sum_{m=1}^{N_c}\sum_{n\in\Psi_m}\log_2\left(1+\frac{\gamma^2\sigma_{m,n}^2P_{m,n}}{N_0W}\right).
\end{aligned}
\tag{8}
$$

where Ψ_m represents the m-th spatial-domain symbol.

On the other hand, only the spatial-domain information is intended for the second user U_2. The spatial-domain mutual information can be expressed as

$$
\begin{aligned}
\mathcal{I}(\mathbf{x}^{\mathrm{i}};\mathbf{y}_2) &= \sum_{m=1}^{N_c}\Pr(\mathbf{x}^{\mathrm{i}}=\Psi_m)\times\int_{\mathbf{y}_2} f(\mathbf{y}_2|\mathbf{x}^{\mathrm{i}}=\Psi_m)\times\\
&\qquad\log_2\left(\frac{f(\mathbf{y}_2|\mathbf{x}^{\mathrm{i}}=\Psi_m)}{f(\mathbf{y}_2)}\right)\mathrm{d}\mathbf{y}_2\\
&= \frac{1}{N_c}\sum_{m=1}^{N_c}\int_{\mathbf{y}_2} f(\mathbf{y}_2|\mathbf{x}^{\mathrm{i}}=\Psi_m)\times\log_2\left(\frac{f(\mathbf{y}_2|\mathbf{x}^{\mathrm{i}}=\Psi_m)}{f(\mathbf{y}_2)}\right)\mathrm{d}\mathbf{y}_2,
\end{aligned}
\tag{9}
$$

where $f(\mathbf{y}_2)$ and $f(\mathbf{y}_2|\mathbf{x}^{\mathrm{i}}=\Psi_m)$ represent the probability density function (PDF) of $\mathbf{y}_2$ and the conditional PDF of $\mathbf{y}_2$, respectively. According to the total probability theorem, the PDF of $\mathbf{y}_2$ can be given as

$$
f(\mathbf{y}_2)=\frac{1}{N_c}\sum_{m=1}^{N_c} f(\mathbf{y}_2|\mathbf{x}^{\mathrm{i}}=\Psi_m). \tag{10}
$$

And the conditional PDF can be further given as

$$
f(\mathbf{y}_2|\mathbf{x}^{\mathrm{i}}=\Psi_m)=\frac{1}{\pi^{N_{2,r}}|\Sigma_m|}\exp(-\mathbf{y}_2^{\mathrm{H}}\Sigma_m^{-1}\mathbf{y}_2), \tag{11}
$$

where Σ_m represents the covariance matrix of $\mathbf{y}_2$ when the spatial-domain symbol $\mathbf{x}^{\mathrm{i}}=\Psi_m$.

B. Lower Bound of the Achievable Rate

In this subsection, we further derive the lower bound of the achievable rate. The achievable rate of the first user U_1 can be expressed as

$$
\begin{aligned}
R_1 &= \frac{W}{2}\times\mathcal{I}(\mathbf{x}^{\mathrm{c}};\mathbf{y}_1|\mathbf{x}^{\mathrm{i}})\\
&= \frac{W}{2N_c}\sum_{m=1}^{N_c}\sum_{n\in\Psi_m}\log_2\left(1+\frac{\gamma^2\sigma_{m,n}^2P_{m,n}}{N_0W}\right).
\end{aligned}
\tag{12}
$$

Since the derived mutual information for the second user U_2 in (9) has no closed form expression, we utilize the Jensen's inequality [22] to derive a lower bound of the achievable rate of U_2, which is shown in (13). Therefore, the lower bound of the achievable rate of the second user U_2 is expressed as

$$
\begin{aligned}
R_2 &= \frac{W}{2}\times\mathcal{I}(\mathbf{x}^{\mathrm{i}};\mathbf{y}_2)\\
&\geq \frac{W}{2}\log_2\left(\frac{N_c}{e^{N_{2,r}}}\right)-\frac{W}{2N_c}\sum_{m=1}^{N_c}\log_2\left(\sum_{t=1}^{N_c}\frac{|\Sigma_m|}{|\Sigma_m+\Sigma_t|}\right).
\end{aligned}
\tag{14}
$$

C. Approximation of the Achievable Rate

In order to obtain a better description of the achievable rate, an approximation is further derived. It can be calculated that the lower bound of the achievable rate of U_2 in (14) approaches $-N_{2,r}W\log_2(e/2)/2$ and $W\log_2(N_c)/2-N_{2,r}W\log_2(e/2)/2$ in the low and high signal to noise ratio (SNR) regions. There exists a constant gap between the lower bound and the true value in the low and high SNR regions, since the true value is supposed to

Authorized licensed use limited to: Tsinghua University. Downloaded on August 27,2020 at 08:36:10 UTC from IEEE Xplore. Restrictions apply.

TABLE I
SIMULATION PARAMETERS

Parameters	Values
Room Size	$5.00\ \text{m} \times 5.00\ \text{m} \times 3.00\ \text{m}$
Location of the LEDs	$(2.00\ \text{m}, 2.00\ \text{m}, 3.00\ \text{m})$ $(2.00\ \text{m}, 3.00\ \text{m}, 3.00\ \text{m})$ $(3.00\ \text{m}, 2.00\ \text{m}, 3.00\ \text{m})$ $(3.00\ \text{m}, 3.00\ \text{m}, 3.00\ \text{m})$
Location of the PDs of U_1	$(2.50\ \text{m}, 2.50\ \text{m}, 0.70\ \text{m})$ $(2.50\ \text{m}, 2.55\ \text{m}, 0.70\ \text{m})$ $(2.55\ \text{m}, 2.50\ \text{m}, 0.70\ \text{m})$ $(2.55\ \text{m}, 2.55\ \text{m}, 0.70\ \text{m})$
Location of the PDs of U_2	$(1.50\ \text{m}, 1.50\ \text{m}, 0.70\ \text{m})$ $(1.50\ \text{m}, 1.55\ \text{m}, 0.70\ \text{m})$
Lambert's mode number of the LEDs	$l = 1$
Area of the PDs	$A_{\text{R}} = 1\ \text{cm}^2$
FOV of the PDs	$\Theta_{1/2} = 60^\circ$
Responsivity of the PDs	$\gamma = 0.25\ \text{A/W}$
Noise power density at the PDs	$N_0 = -180\ \text{dBm}$ [23]
Modulation Bandwidth	$W = 20\ \text{MHz}$

be 0 and $W\log_2(N_c)/2$. Thus, we apply a constant shift of $N_{2,r}W\log_2(e/2)/2$ to derive an approximation of the achievable rate of U_2, which is

$$R_2 \approx \frac{W}{2}\log_2\left(\frac{N_c}{2^{N_{2,r}}}\right) - \frac{W}{2N_c}\sum_{m=1}^{N_c}\log_2\left(\sum_{t=1}^{N_c}\frac{|\Sigma_m|}{|\Sigma_m+\Sigma_t|}\right). \tag{15}$$

Therefore, the approximation of the sum rate of the users U_1 and U_2 can be expressed as

$$\begin{aligned} R =& R_1 + R_2 \\ \approx& \frac{W}{2N_c}\sum_{m=1}^{N_c}\sum_{n\in\Psi_m}\log_2\left(1+\frac{\gamma^2\sigma_{m,n}^2 P_{m,n}}{N_0 W}\right) + \\ & \frac{W}{2}\log_2\left(\frac{N_c}{2^{N_{2,r}}}\right) - \frac{W}{2N_c}\sum_{m=1}^{N_c}\log_2\left(\sum_{t=1}^{N_c}\frac{|\Sigma_m|}{|\Sigma_m+\Sigma_t|}\right). \end{aligned} \tag{16}$$

V. SIMULATION RESULTS

We consider a cubic room with $N_t = 4$ LEDs located at the center of the ceiling. Two user devices, U_1 with $N_{1,r} = 4$ PDs and U_2 with $N_{2,r} = 2$ PDs are supported in the indoor VLC system. U_1 is a smart electronic device with high data rate demands, and U_2 is an IoT device with low QoS requirements. The detailed simulation parameters are provided in Table I. Although only the results of the one-user-group scenario is provided in this section, it can easily extended to the multi-user-group scenarios since orthogonal resource allocation is adopted among user groups.

Firstly, the accuracy and the efficiency of the proposed approximations of the SIC-free NOMA scheme is evaluated. In Fig. 3, the exact values through Monte-Carlo methods, the proposed approximations, and the derived lower bounds of

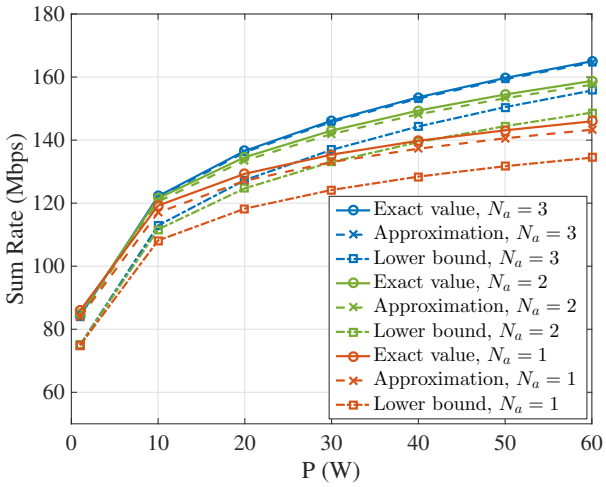


Fig. 3. The exact values, the proposed approximations, and the derived lower bounds of the achievable sum rates with different numbers of activated LEDs and total transmit electrical power.

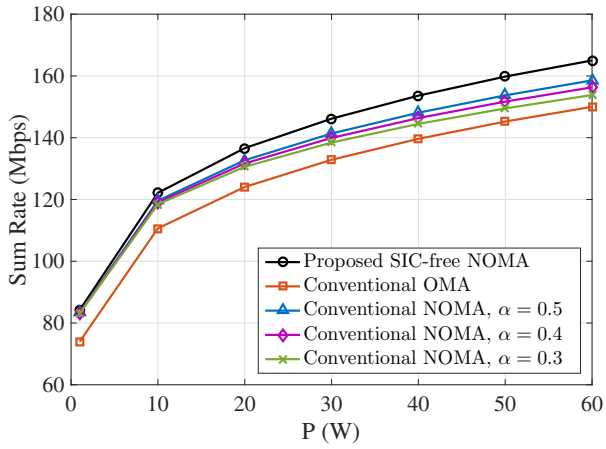


Fig. 4. Comparisons of the achievable sum rates of the proposed SIC-free NOMA scheme and conventional multiple access schemes.

the achievable sum rates are illustrated as solid lines, dotted lines, and dash-dotted lines, respectively. It can be seen that the lower bounds can track the trends of the exact values with constant gaps. And the further proposed approximations of the sum achievable rates are very close to the exact values under all the simulated situations, which shows the proposed approximation can provide an efficient calculation of the achievable sum rate with high accuracy.

Then, we compare the achievable sum rate of the proposed scheme with the state-of-the-art multiple access schemes. The achievable sum rates of the conventional NOMA scheme [24] and OMA scheme are illustrated as benchmarks. In the conventional NOMA scheme, the signals for different users are allocated with different power levels and are superimposed on top of each other. SIC detectors are utilized at the receivers to decode the signals for different users. Specifically, αP is allocated to U_1 and $(1-\alpha)P$ is allocated

Authorized licensed use limited to: Tsinghua University. Downloaded on August 27,2020 at 08:36:10 UTC from IEEE Xplore. Restrictions apply.

to U_2, respectively. In the OMA scheme, different users are allocated with different frequency ranges. In the simulated OMA scheme, we allocate $0.8P$ power and $0.8W$ bandwidth to U_1, and $0.2P$ power and $0.2W$ bandwidth to U_2. In the proposed NOMA scheme, we activate $N_a = 3$ LEDs to transmit information at the same time. We assume the channel state information of the users are not known at the transmitter. Thus, no extra precoding is applied. It can be seen from Fig. 4 that the proposed SIC-free NOMA scheme enjoys the highest achievable sum rate in all the simulated scenarios. The proposed scheme achieves better performance than the OMA scheme mainly because of the non-orthogonal resource allocations. The proposed scheme outperforms the conventional NOMA schemes because in the conventional NOMA scheme, more power is allocated to the IoT user U_2 with poor channel condition to achieve successful signal detection at U_2, which is more than what it actually needs and causes less power allocation for U_1. Moreover, the intra-group interference are canceled completely and the SIC is avoided in the proposed scheme to reduce signal detection complexity.

VI. Conclusion

In this paper, a novel SIC-free NOMA scheme has been proposed for users with diverse QoS requirements in the indoor VLC systems, especially the smart electronic devices with high data rate demands and IoT devices with low data rate requirements. The information bits intended for the users in the same group are conveyed through spatial-domain symbols and constellation-domain symbols, respectively, to cancel the intra-group interference and avoid the complicated SIC at receivers. A closed form approximation of the achievable rate has been derived to provide efficient estimation of the achievable rate of the proposed scheme. The benefits of the proposed scheme has been validated through theoretical analyses and simulations.

Acknowledgement

This work is based upon the research supported by the Natural Science Foundation of Guangdong Province (Grant No. 2015A030312006), the National Natural Science Foundation of China (Grant No. 61871255), the National Key Research and Development Program of China (Grant No.2017YFE0113300), and the Fok Ying-Tung Education Foundation.

References

[1] D. Karunatilaka, F. Zafar, V. Kalavally, and R. Parthiban, "LED based indoor visible light communications: State of the art," *IEEE Commun. Surveys Tuts.*, vol. 17, no. 3, pp. 1649–1678, Mar. 2015.

[2] Z. Ding, X. Lei, G. K. Karagiannidis, R. Schober, J. Yuan, and V. K. Bhargava, "A survey on non-orthogonal multiple access for 5G networks: Research challenges and future trends," *IEEE J. Sel. Areas Commun.*, vol. 35, no. 10, pp. 2181–2195, Oct. 2017.

[3] T. Wang, J. Tan, W. Ding, Y. Zhang, F. Yang, J. Song, and Z. Han, "Intercommunity detection scheme for social Internet of Things: Compressive sensing over graphs approach," *IEEE Internet Things J.*, vol. 5, no. 6, pp. 4550–4557, Dec. 2018.

[4] A. Jovicic, J. Li, and T. Richardson, "Visible light communication: opportunities, challenges and the path to market," *IEEE Commun. Mag.*, vol. 51, no. 12, pp. 26–32, Dec. 2013.

[5] M. Shafi, A. F. Molisch, P. J. Smith, T. Haustein, P. Zhu, P. De Silva, F. Tufvesson, A. Benjebbour, and G. Wunder, "5G: A tutorial overview of standards, trials, challenges, deployment, and practice," *IEEE J. Sel. Areas Commun.*, vol. 35, no. 6, pp. 1201–1221, Jun. 2017.

[6] Y. Saito, Y. Kishiyama, A. Benjebbour, T. Nakamura, A. Li, and K. Higuchi, "Non-orthogonal multiple access (NOMA) for cellular future radio access," in *IEEE 77th Vehicular Technology Conference (VTC Spring)*, Dresden, Germany, Jun. 2013.

[7] R. C. Kizilirmak, C. R. Rowell, and M. Uysal, "Non-orthogonal multiple access (NOMA) for indoor visible light communications," in *4th International Workshop on Optical Wireless Communications (IWOW)*, Istanbul, Turkey, Sep. 2015, pp. 98–101.

[8] C. Chen, W. Zhong, H. Yang, and P. Du, "On the performance of MIMO-NOMA-based visible light communication systems," *IEEE Photon. Technol. Lett.*, vol. 30, no. 4, pp. 307–310, Feb. 2018.

[9] T. Fath and H. Haas, "Performance comparison of MIMO techniques for optical wireless communications in indoor environments," *IEEE Trans. Commun.*, vol. 61, no. 2, pp. 733–742, Feb. 2013.

[10] C. R. Kumar and R. K. Jeyachitra, "Power efficient generalized spatial modulation MIMO for indoor visible light communications," *IEEE Photon. Technol. Lett.*, vol. 29, no. 11, pp. 921–924, Jun. 2017.

[11] T. Wang, F. Yang, L. Cheng, and J. Song, "Spectral-efficient generalized spatial modulation based hybrid dimming scheme with LACO-OFDM in VLC," *IEEE Access*, vol. 6, pp. 41 153–41 162, Jun. 2018.

[12] K. Cai and M. Jiang, "SM/SPPM aided multiuser precoded visible light communication systems," *IEEE Photon. J.*, vol. 8, no. 2, pp. 1–9, Apr. 2016.

[13] T. Wang, F. Yang, and J. Song, "Novel index modulation aided non-orthogonal multiple access for visible light communication," in *IEEE Global Communications Conference (GLOBECOM)*, Waikoloa, HI, Dec. 2019.

[14] T. Wang, F. Yang, C. Pan, L. Cheng, and J. Song, "Spectral-efficient hybrid dimming scheme for indoor visible light communication: A subcarrier index modulation based approach," *J. Lightw. Technol.*, vol. 37, no. 23, pp. 5756–5765, Dec. 2019.

[15] F. Yang, J. Gao, and S. Liu, "Novel visible light communication approach based on hybrid OOK and ACO-OFDM," *IEEE Photon. Technol. Lett.*, vol. 28, no. 14, pp. 1585–1588, Jul. 2016.

[16] K. Lee, H. Park, and J. R. Barry, "Indoor channel characteristics for visible light communications," *IEEE Commun. Lett.*, vol. 15, no. 2, pp. 217–219, Feb. 2011.

[17] Y. Sun, F. Yang, and J. Gao, "Comparison of hybrid optical modulation schemes for visible light communication," *IEEE Photon. J.*, vol. 9, no. 3, Jun. 2017.

[18] X. Zhang, Q. Gao, C. Gong, and Z. Xu, "User grouping and power allocation for NOMA visible light communication multi-cell networks," *IEEE Commun. Lett.*, vol. 21, no. 4, pp. 777–780, Apr. 2017.

[19] M. S. Ali, H. Tabassum, and E. Hossain, "Dynamic user clustering and power allocation for uplink and downlink non-orthogonal multiple access (NOMA) systems," *IEEE Access*, vol. 4, pp. 6325–6343, Aug. 2016.

[20] J. Wang, H. Ge, J. Zhu, J. Wang, J. Dai, and M. Lin, "Adaptive spatial modulation for visible light communications with an arbitrary number of transmitters," *IEEE Access*, vol. 6, pp. 37 108–37 123, Jun. 2018.

[21] Z. An, J. Wang, J. Wang, and J. Song, "Mutual information and error probability analysis on generalized spatial modulation system," *IEEE Trans. Commun.*, vol. 65, no. 3, pp. 1044–1060, Mar. 2017.

[22] L. He, J. Wang, and J. Song, "Spectral-efficient analog precoding for generalized spatial modulation aided mmWave MIMO," *IEEE Trans. Veh. Technol.*, vol. 66, no. 10, pp. 9598–9602, Oct. 2017.

[23] I. Stefan, H. Burchardt, and H. Haas, "Area spectral efficiency performance comparison between VLC and RF femtocell networks," in *IEEE International Conference on Communications (ICC)*, Budapest, Hungary, Jun. 2013, pp. 3825–3829.

[24] Y. Liu, G. Pan, H. Zhang, and M. Song, "On the capacity comparison between MIMO-NOMA and MIMO-OMA," *IEEE Access*, vol. 4, pp. 2123–2129, May 2016.

Authorized licensed use limited to: Tsinghua University. Downloaded on August 27,2020 at 08:36:10 UTC from IEEE Xplore. Restrictions apply.